Electronic Supplementary Information

ZnO nanowire arrays with *in situ* sequentially self-assembled vertically oriented CdS nanosheets as superior photoanodes for photoelectrochemical water splitting

Chunmei Li [a,b], Hua Lin [c], Maoxiang Jing [d], Lian Ying Zhang [e], Weiyong Yuan [a,f,*], Chang Ming Li [c]

[a] *Ningbo Research Institute, Zhejiang University, Ningbo 315100, China*

[b] *School of Optoelectronic Science and Engineering, University of Electronic Science and Technology of China, Chengdu 611731, China*

[c] *School of Materials & Energy, Southwest University, Chongqing 400715, China*

[d] *Institute for Advanced Materials, School of Materials Science & Engineering, Jiangsu University, Zhenjiang 212013, China*

[e] *Institute of Materials for Energy and Environment, College of Materials Science and Engineering, Qingdao University, Qingdao 266071, China*

[f] *College of Chemical and Biological Engineering, Zhejiang University, Hangzhou 310027, China*

* *Corresponding Author. Tel./ fax: +86 574 88229995. E-mail: wyyuan@zju.edu.cn*

Contents

11. Mott−Schottky plots of ZnO NWA, ZnO NW@ZnO NP array, ZnO NW@CdS NP array, and ZnO NW@CdS NS array obtained at frequencies of 800, 1000, and 1200 Hz in the dark (Figure S6).

12. Nyquist and Bode plots of ZnO NWAs, ZnO NW@ZnO NP arrays, ZnO NW@CdS NP arrays, and ZnO NW@CdS NS arrays in dark (Figure S7).

13. Chronoamperometric curve of ZnO NW@CdS NS array after 50 on/off cycles of solar irradiation and LSV curves of ZnO NW@CdS NS array before and after 50 cycles (Figure S8).

14. FESEM image of ZnO NW@CdS NS array after the stability test (Figure S9).

1. Calculation of photoconversion efficiency

The photoconversion efficiency of a photoanode was calculated according to the following formula:[1-2]

$$\eta\% = \frac{J(1.23 - V)}{P} \times 100$$

Where J is the current density under simulated sunlight irradiation, V is the applied voltage versus RHE, and P is the light intensity (100 mW•cm^{-2}).

2. Calculation of flatband potential and donor density

The depletion layer capacitance obtained from the electrochemical impedance spectra can be described by the Mott−Schottky equation:[1,3]

$$\frac{1}{C^2} = \frac{2}{e_0 \varepsilon \varepsilon_0 N_d}[(V - V_{FB}) - \frac{kT}{e_0}]$$

where e_0 is the electron charge, ε the dielectric constant of ZnO (since the samples are ZnO and ZnO modified with thin layer of CdS, we assume that their dielectric constants are the same [4-6]), ε_0 the permittivity of vacuum (8.85×10^{-12} N^{-1}C^{2}m^{-2}), N_d the donor density, V the electrode applied potential, V_{FB} the flatband potential, and $\frac{kT}{e_0}$ is a temperature-dependent correction term. Therefore, V_{FB} can be determined from the intersection point between the extrapolated linear line and x-axis in Mott−Schottky (M-S) plots ($\frac{1}{C^2}$ versus V) and N_d can be estimated from the slope of the M-S plots according to the following equation:[1,3]

$$N_d = \frac{2}{e_0 \varepsilon \varepsilon_0} \left[\frac{d\frac{1}{C^2}}{dV} \right]^{-1}$$

3. Calculation of Debye length

The charge carrier diffusion lengths (Debye length, L_D) for both electrodes were also calculated according to the following equation:[1,7]

$$L_D = \left(\frac{\varepsilon \varepsilon_0 kT}{e^2 N_D} \right)^{\frac{1}{2}}$$

where k is the Boltzmann constant (1.38×10^{-23} J K^{-1}) and T is the absolute temperature (K).

4. Calculation of depletion layer width

The depletion layer width (W) at 0.0 V vs. SCE can be calculated via the following equation:[1,7]

$$W = \left(\frac{2\varepsilon \varepsilon_0 \phi}{e^2 N_D} \right)^{\frac{1}{2}}$$

where $\phi = V - V_{FB}$ $\phi = V - V_{FB}$ is the maximum potential drop in the depletion layer. A potential of 0.0 V was chosen because of the negligible dark current at that potential.
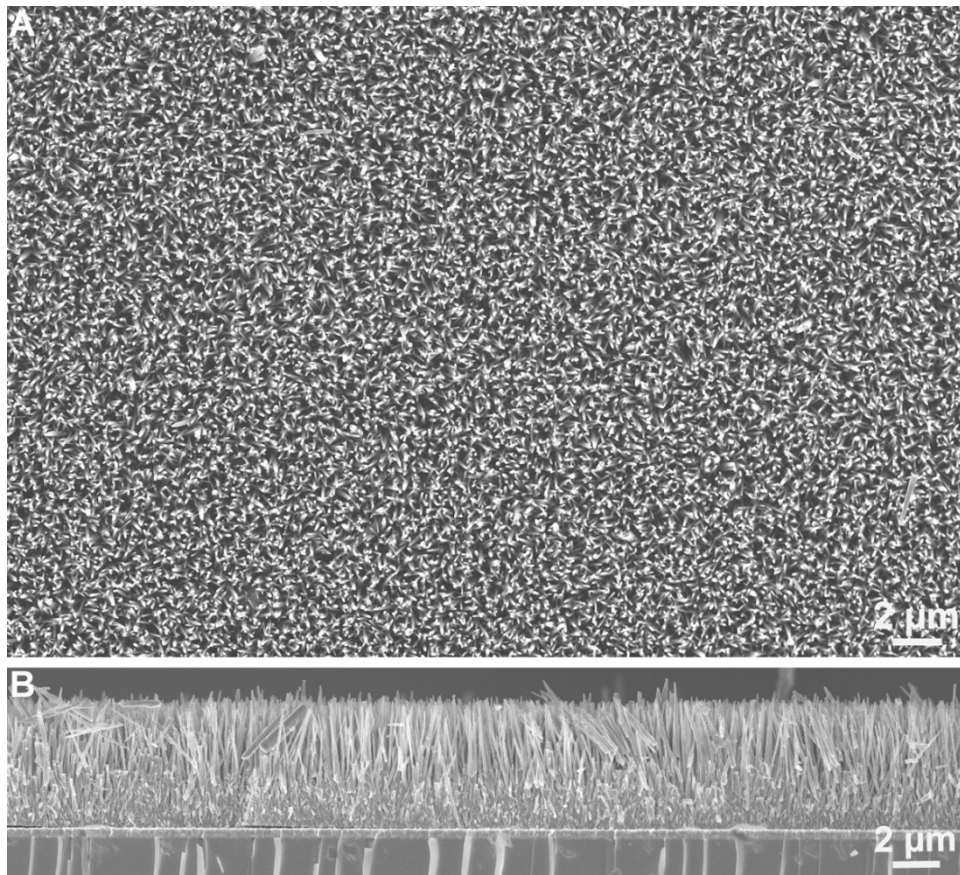
Figure S1. Large-area top-view (A) and cross-section (B) FESEM images of ZnO NWAs.
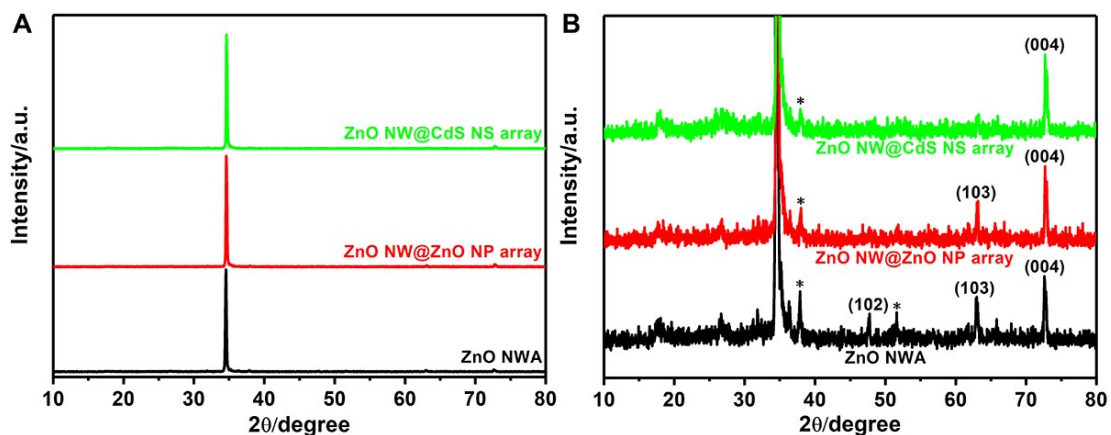

Figure S2. XRD patterns (A) and their enlarged ones (B) of ZnO NWA, ZnO NW@ZnO NP array, and ZnO NW@CdS NS array.
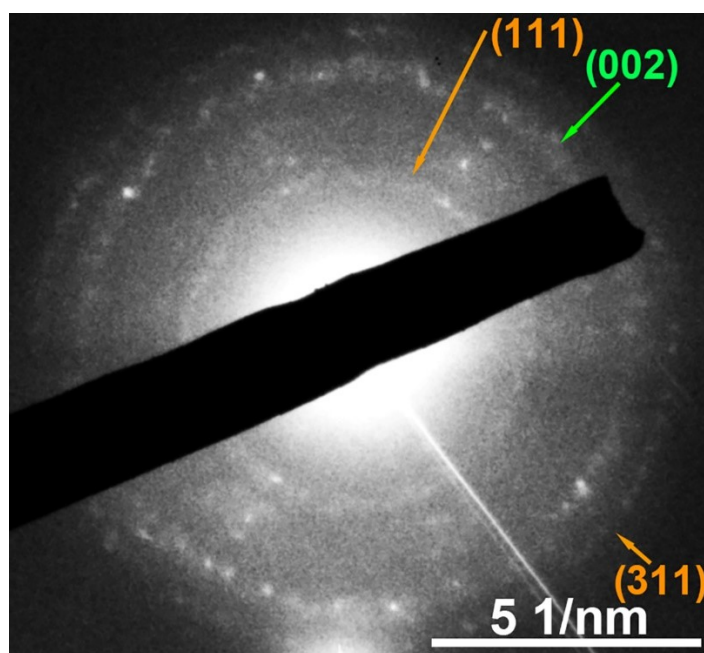

Figure S3. SAED pattern of ZnO NW@CdS NS array. Brown and green colors represent the crystal planes of CdS (JPCDS 80-0019) and hexagonal wurtzite ZnO, respectively.
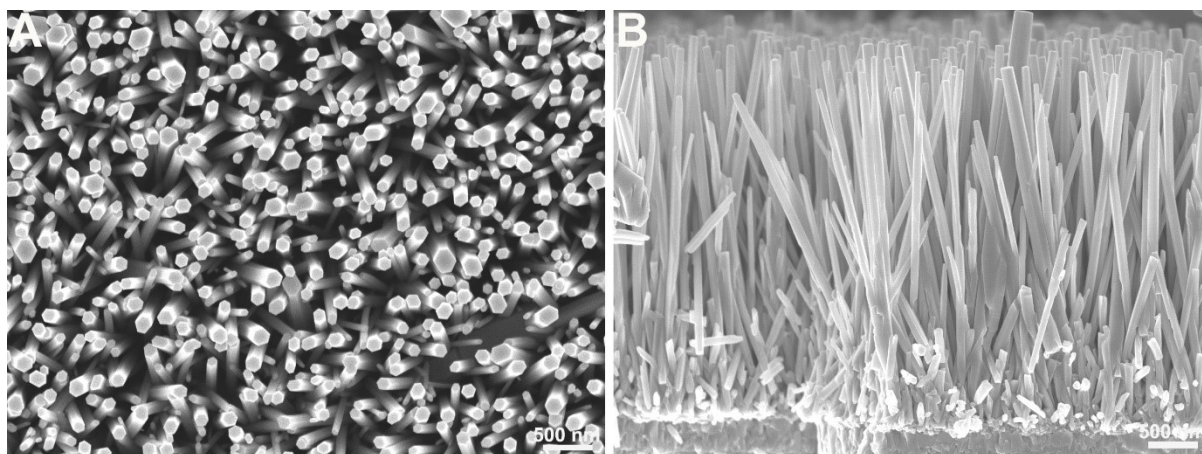
Figure S4. Top-view (A) and cross-section (B) FESEM images of ZnO NWAs grown without the assistance of PEI.
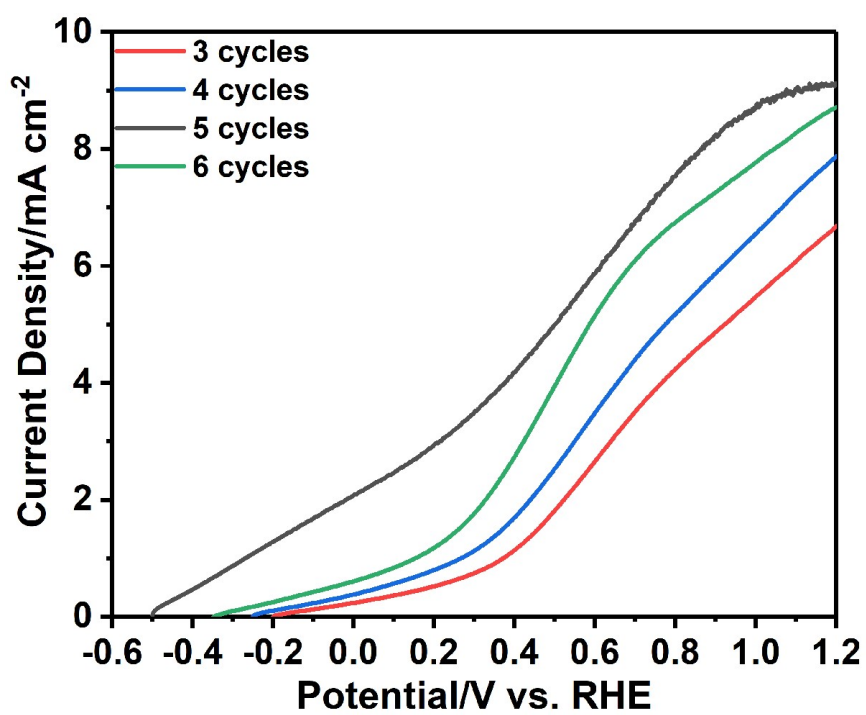

Figure S5. Linear sweep voltammograms of ZnO NW@CdS NS with different deposition cycle numbers.

Table S1. PEC performance of representative ZnO-based photoanodes for water splitting.

| Photoanode	Photocurrent density	Onset potential	Maximum photoconversion Efficiency	Light source used	Electrolyte	Ref.
ZnO/CdS core/shell nanowire arrays	7.23 mA cm^{-2} (0 V vs. SCE)	-1.55 V (vs. SCE)	3.53%	AM 1.5 G, 100 mW cm^{-2}	1 M Na_2S	8
ZnO/CdTe Core-Shell Nanocable Arrays	~5.9 mA cm^{-2} (0 V vs. SCE)	-0.8 V (vs. SCE)		AM 1.5 G, 100 mW cm^{-2}	0.5 M S and 0.3 M Na_2S	9
CdSe/ZnO with double layered tubular structure	2.55 mA cm^{-2} (0 V vs. Ag/AgCl)	-1.1 V (vs. Ag/AgCl)	1.78%	500 W Xe lamp, 100 mW cm^{-2}	0.1 M Na_2S	10
ZnO/GaON nanowire arrays	2.25 mA cm-2 (1.23 V vs. RHE)	~0.1 V (vs. RHE)	0.85%	500 W Xe lamp, 100 mW cm^{-2}	0.5 M KOH	11
CdS NP/ZnO NW heterostructure arrays	~4.5 mA cm^{-2} (0 V vs. SCE)	~-1.3 V (vs. SCE)		AM 1.5 G, 100 mW cm^{-2}	1 M Na_2S	12
3D-branched ZnO NWA–CdS nanoparticle composite	3.58 mA cm^{-2} (0 V vs. Ag/AgCl)		3.1%	70 mW cm^{-2}	0.5 M Na_2S	13
ZnO@Au@ZIF-67	1.93 mA cm^{-2} (0.6 V vs. SCE)	-0.1 V (vs. SCE)	0.8%	150 W Xe lamp, 100 mW cm^{-2}	0.5 M Na_2SO_4	14
3D ZnO/TiO$_2$/FeOOH	1.59 mA cm^{-2} (1.8 V vs. RHE)	0.14 V (vs. RHE)	0.36%	AM 1.5 G, 100 mW cm^{-2}	0.5 M Na_2SO_4	15
composition-graded Zn$_x$Cd$_{1-x}$Se@ZnO core-shell nanowire array	~7.4 mA cm^{-2} (1.23 V vs. RHE)	-1.2 V (vs. Ag/AgCl)		AM 1.5 G, 100 mW cm^{-2}	0.35 M Na_2SO_3 and 0.24 M Na_2S	16
BiVO4/ZnO QDs	~5.8 mA cm-2 (1.23 V vs. RHE)	~0.23 V (vs. RHE)	1.75%	AM 1.5 G, 100 mW cm^{-2}	0.1 M Na_2SO_4	17
ZnO@InP QD	1.2 mA cm^{-2} (1.0 V vs. Ag/AgCl)		~1.3%	AM 1.5 G, 100 mW cm^{-2}	0.5 M Na_2SO_4	18
LDH/LFO/ZnO	2.46 mA cm^{-2} (1.23 V vs. RHE)	0.31 V (vs. RHE)	0.76%	AM 1.5 G, 100 mW cm^{-2}	0.5 M Na_2SO_4	19
ZnO-CdS core-shell nanocable array	6.0 mA cm^{-2}	-1.3 V (vs. Ag/AgCl)		AM 1.5 G, 100 mW cm^{-2}	1 M Na_2S	20
Al-ZnO/CdS/TiO$_2$	11.7 mA cm^{-2}	~-0.3 V (vs. RHE)	5.9%	AM 1.5 G, 100 mW cm^{-2}	0.25 M Na_2S and 0.35 M Na_2SO_3	21
Al-ZnO/CdS/Al$_2$O$_3$	10.4 mA cm^{-2}	~-0.2 V (vs. RHE)	5.75%	AM 1.5 G, 100 mW cm^{-2}	0.25 M Na_2S and 0.35 M Na_2SO_3	22
ZnO–ZnS solid solution nanowire arrays	1.5 mA cm^{-2} (1 V vs. Ag/AgCl)	-0.7 V (vs. Ag/AgCl)		AM 1.5 G, 100 mW cm^{-2}	0.5 M Na_2S and K_2SO_3 solution	23
NiOOH/ZnWO$_4$/ZnO	1.7 mA cm^{-2} (1.23 V vs. RHE)	~0.4 V (vs. RHE)	0.46%	AM 1.5 G, 100 mW cm^{-2}	0.02 M KOH	24
ZnO@CdTe	2.0 mA cm^{-2} (1.0 V vs. Ag/AgCl)		1.83%	AM 1.5 G, 100 mW cm^{-2}	0.5 M Na_2SO_4	25
ZnO/CdS/CuSbS$_2$	6.42 mA cm-2 (0 V vs. Ag/AgCl)	-1.1 V vs. Ag/AgCl		AM 1.5 G, 100 mW cm^{-2}	0.35 M Na_2SO_3 and 0.25 M Na_2S	26
ZnO NW@CdS NS array	9.10 mA cm^{-2} (1.23 V vs. RHE)	-0.5 V (vs. RHE)	3.72%	AM 1.5 G, 100 mW cm^{-2}	0.2 M Na_2S	This work
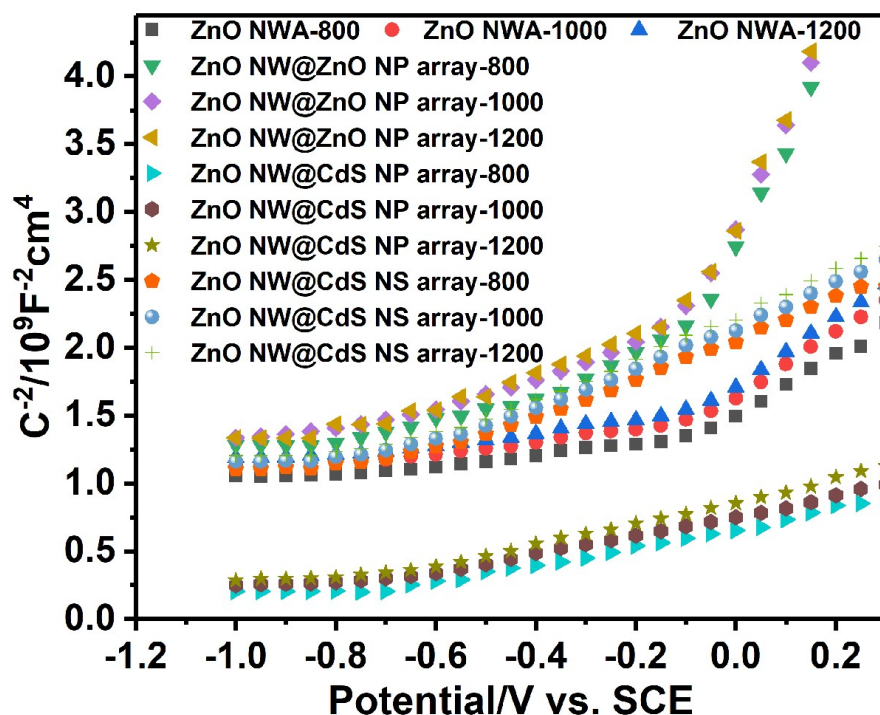
Figure S6. Mott−Schottky plots of ZnO NWA, ZnO NW@ZnO NP array, ZnO NW@CdS NP array, and ZnO NW@CdS NS array obtained at frequencies of 800, 1000, and 1200 Hz in the dark.
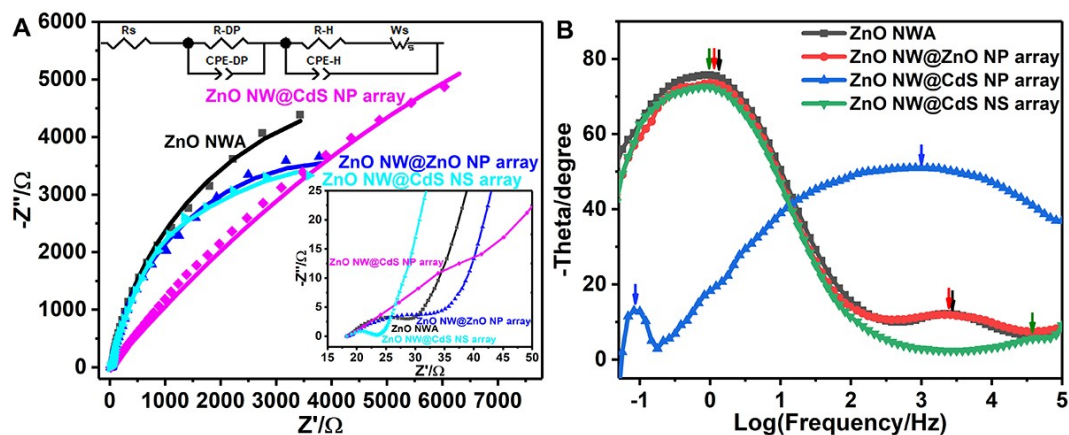

Figure S7. Nyquist (A) and Bode (B) plots of ZnO NWAs, ZnO NW@ZnO NP arrays, ZnO NW@CdS NP arrays, and ZnO NW@CdS NS arrays in dark. The inset in the lower right corner of (A) shows Nyquist plots at the high-frequency region, and the one in the upper left corner shows the equivalent circuit used for simulation.
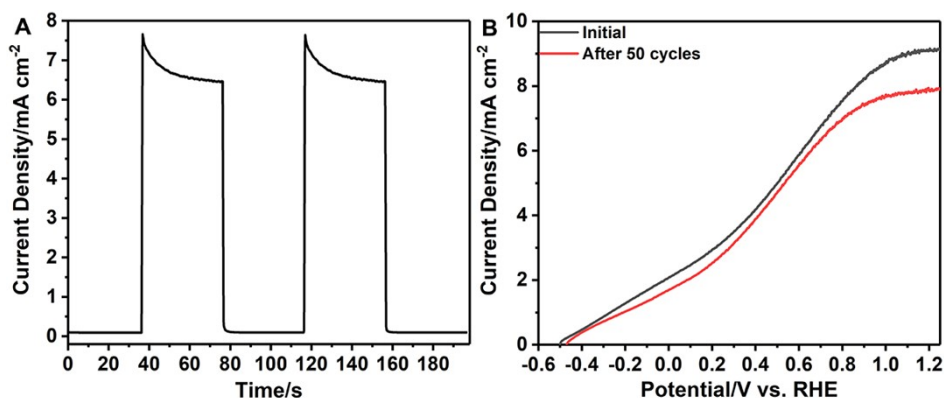
Figure S8. (A) Chronoamperometric curve of ZnO NW@CdS NS array after 50 on/off cycles of solar irradiation. (B) LSV curves of ZnO NW@CdS NS array before and after 50 cycles.
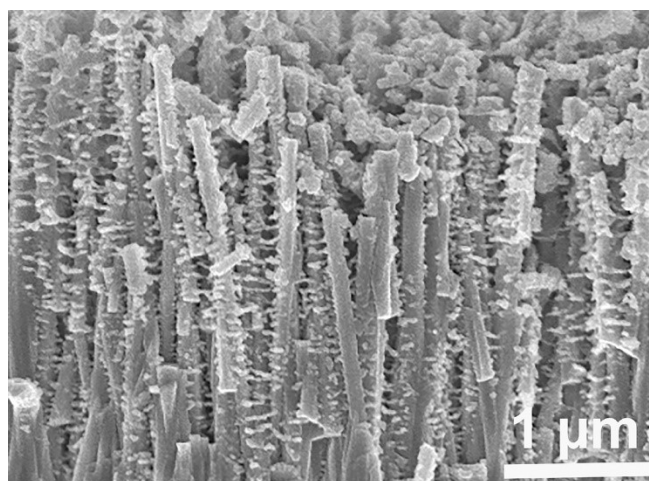

Figure S9. FESEM image of ZnO NW@CdS NS array after the stability test.

References

[1] W. Yuan, J. Yuan, J. Xie, C. M. Li, *ACS Appl. Mater. Interfaces* **2016**, *8*, 6082.
[2] Z. Li, W. Luo, M. Zhang, J. Feng, Z. Zou, *Energy Environ. Sci.* **2013**, *6*, 347.
[3] K. Gelderman, L. Lee, S. W. Donne, *J. Chem. Educ.* **2007**, *84*, 685.
[4] A. Ghobadi, T. G. U. Ghobadi, F. Karadas, E. Ozbay, *Sci. Rep.* **2018**, *8*, 16322.
[5] F. Malara, A. Minguzzi, M. Marelli, S. Morandi, R. Psaro, V. D. Santo, A. Naldoni, *ACS Catal.* **2015**, *5*, 5292.
[6] Q. Rui, L. Wang, Y. Zhang, C. Feng, B. Zhang, S. Fu, H. Guo, H. Hu, Y. Bi, *J. Mater. Chem. A* **2018**, *6*, 7021.
[7] C. Fàbrega, D. Monllor-Satoca, S. Ampudia, A. Parra, T. Andreu, J. R. Morante, *J. Phys. Chem. C* **2013**, *117*, 20517.
[8] Y. Tak, S. J. Hong, J. S. Lee, K. Yong, *J. Mater. Chem.* **2009**, *19*, 5945.
[9] X. N. Wang, H. J. Zhu, Y. M. Xu, H. Wang, Y. Tao, S. Hark, X. D. Xiao, Q. A. Li, *ACS Nano* **2010**, *4*, 3302.
[10] M. Wang, J. G. Jiang, G. J. Liu, J. W. Shi, L. J. Guo, *Appl. Catal. B* **2013**, *138*, 304.

[11] H. P. Ma, J. H. Yang, J. J. Tao, K. P. Yuan, P. H. Cheng, W. Huang, J. C. Wang, Q. X. Guo, H. L. Lu, D. W. Zhang, *Nano Energy* **2019**, *66*, 104089.

[12] Y. Tak, S. J. Hong, J. S. Lee, K. Yong, *Cryst. Growth Des.* **2009**, *9*, 2627.

[13] Z. Bai, X. Yan, Y. Li, Z. Kang, S. Cao, Y. Zhang, *Adv. Energy Mater.* **2016**, *6*, 1501459.

[14] Y. Dou, J. Zhou, A. Zhou, J.-R. Li, Z. Nie, *J. Mater. Chem. A* **2017**, *5*, 19491.

[15] Z. Li, S. Feng, S. Liu, X. Li, L. Wang, W. Lu, *Nanoscale* **2015**, *7*, 19178.

[16] H. Li, C. Cheng, X. Li, J. Liu, C. Guan, Y. Tay, H. Fan, *J. Phys. Chem. C* **2012**, *116*, 3802.

[17] J. Li, H. Yuan, J. Li, W. Zhang, Y. Liu, N. Liu, H. Cao, Z. Jiao, *Appl. Catal. B* **2021**, *285*, 119833.

[18] H. M. Chen, C. K. Chen, C. C. Lin, R. S. Liu, H. Yang, W. S. Chang, K. H. Chen, T. S. Chan, J. F. Lee, D. P. Tsai, *J. Phys. Chem. C* **2011**, *115*, 21971.

[19] X. Long, C. Wang, S. Wei, T. Wang, J. Jin, J. Ma, *ACS Appl. Mater. Interfaces* **2020**, *12*, 2452.

[20] Y. Myung, D. M. Jang, T. K. Sung, Y. J. Sohn, G. B. Jung, Y. J. Cho, H. S. Kim, J. Park, *ACS Nano* **2010**, *4*, 3789.

[21] R. Wang, L. Wang, Y. Zhou, Z. Zou, *Appl. Catal. B* **2019**, *255*, 117738.

[22] R. Wang, X. Li, L. Wang, X. Zhao, G. Yang, A. Li, C. Wu, Q. Shen, Y. Zhou, Z. Zou, *Nanoscale* **2018**, *10*, 19621.

[23] H. M. Chen, C. K. Chen, R. S. Liu, C. C. Wu, W. S. Chang, K. H. Chen, T. S. Chan, J. F. Lee, D. P. Tsai, *Adv. Energy Mater.* **2011**, *1*, 742.

[24] S. Fu, H. Hu, C. Feng, Y. Zhang, Y. Bi, *J. Mater. Chem. A* **2019**, *7*, 2513.

[25] H. Chen, C. Chen, Y.C. Chang, C. W. Tsai, R. S. Liu, S. F. Hu, W.S. Chang, K.H. Chen, *Angew. Chem. Int. Ed.* **2010**, *49*, 5966.

[26] R. R. Su, Y. X. Yu, Y. H. Xiao, X. F. Yang, W. D. Zhang, *Int. J. Hydrog. Energy* **2018**, *43*, 6040.